Preliminary code development of pool scrubbing phenomenon in two regions

Yo Han Kim, Dong Hoon Kam, Yong Hoon Jeong*
Department of Nuclear and Quantum Engineering, Korea Advanced Institute of Science and Technology, 291, Daehak-ro, Yuseong-gu, Daejeon, 305-701, Republic of Korea
**Corresponding author: jeongyh@kaist.ac.kr*

1. Introduction

Regulations on nuclear power plants have been strengthened since the Fukushima NPP accident. The severe accident regulation requires that the cumulative frequency of accidents with cesium emission higher than 100 TBq is less than 1.0E-06/Rx year [1]. The integrity of containment should be ensured to prevent the release of radioactive nuclides. However, if bypass accident like SGTR and ISLOCA occurs, the radioactive materials are directly released into the environment even if the integrity of the containment is ensured. Protection of public health and minimization of environmental pollution should be realized even under such accidents. Therefore, a release of radioactive material should be minimized, and it is also crucial to accurately estimate the amount of radioactive material released. In this paper, decontamination factors(DF) during the pool scrubbing process were calculated. For the purpose, pool scrubbing code was developed and the calculated results have been compared with POSEIDON-II experiments.

2. Methods

Pool scrubbing is a phenomenon in which aerosols in a gas bubble are trapped at the interface between bubble gas and fluid. In this section, main correlations used to model the pool scrubbing phenomenon are described. The pool scrubbing effect can be considered in two regions: injection region and bubble rising region.

2.1 Injection region

A globule is formed due to an injection of gas containing the aerosols at the injection region. The globule is very unstable, so it breaks up into many small bubbles and become stable. In this part, the aerosols are removed due to the inertial impaction and rapid injection rate but also are removed by other mechanisms.

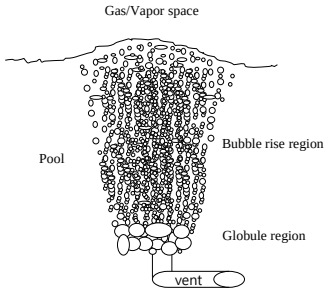

Fig 1. Schematic diagram of pool scrubbing

2.1.1 Globule formation

The formation of a globule is strongly related to the velocity of the inlet gas and the orifice diameter. For a vertical orifice case, Initial globule volume can be expressed as follow [2]:

$$V_{Globule} = 0.0505(1000U_o)^{0.95}(1000D_o)^{2.38}10^{-9} \quad (1)$$

2.1.2 Aerosol removal at the injection region

There are five main removal mechanisms at the injection part. Inertial impaction occurs when fast gas collides with stationary liquid. When the gas exits the outlet vent at high speed, the initial globule loses its velocity quickly. During the process, the forward globule interface can capture particles as it slows down and stops. Decontamination factor made by inertial impaction can be defined as a function of Stokes number [2]:

$$DF_{Inj_{imp}}(Stk) = \frac{1}{1-\alpha(Stk)} \quad (2)$$

$$Stk = \frac{\rho_p U_o d_p^2}{18\mu_g l} \quad (3)$$

As the globule breaks at the pool, DF for steam condensation mechanism can be expressed as a ratio between saturation water pressures [3].

$$DF_{Inj_{con}} = \frac{X_o}{X_i} \quad (4)$$

Each of depositions by centrifugal, diffusional and gravitational forces in the globule are divided into two regions [3]: injection and detachment.

$$DF_{Inj_{cen}} = DF_{cen_{inj}} \times DF_{cen_{det}} = e^{\frac{U_c}{U_{inlet}}} \times e^{\frac{U_o U_g \rho_g}{9 D_o f g \rho_l}} \quad (5)$$

$$DF_{Inj_{dif}} = DF_{dif_{inj}} \times DF_{dif_{det}} = e^{\frac{16}{3D_o}\sqrt{\frac{Dt_f}{\pi}}} \times e^{\frac{12}{D_o}\sqrt{\frac{D}{\pi D_o}}\frac{4\rho_l D_g}{3\rho_g f}\left[\left(\frac{3\rho_g{}^2}{4\rho_l{}^2 U_o}+\frac{1}{U_o}\right)^{0.5}-\left(\frac{1}{U_o}\right)^{0.5}\right]} \quad (6)$$

$$DF_{Inj_{cen}} = DF_{cen_{inj}} \times DF_{cen_{det}} = e^{\frac{6A_s U_g t_{stop}}{\pi D_g{}^3}} \times e^{\frac{3U_g t_{stop}}{2D_g}} \quad (7)$$

2.1.3 Globule breakup

As a globule rises, it becomes unstable and split into many stable small bubbles. There are three representative criteria for a globule breakup. Weber criterion and Levich criterion are used in BUSCA code and Battelle breakup criterion is used in SPARC code. In the Weber criterion, if the Weber number becomes greater than 15, a globule breaks. The Levich criterion tells that a globule breaks when its internal dynamic pressure exceeds the forces of surface tension [4]. The Battelle breakup occurs when a globule travels a distance 10 times the initial globule diameter. Breakup criteria can be expressed as critical diameters [5]:

$$D_{cr_{Weber}} = 15\frac{\sigma}{{U_b}^2}\frac{1}{\rho_l} \quad (8)$$

$$D_{cr_{Levich}} = \frac{\sigma}{{U_b}^2}\left(\frac{12}{\rho_g{\rho_l}^2}\right)^{\frac{1}{3}} \quad (9)$$

$$D_{cr_{Battelle}} = 10\mathrm{D}_{G_{initial}} \quad (10)$$

2.2 Bubble rising region

Small bubbles generated from the globule rise until they reach the surface of the water. Aerosols in the bubbles are removed by five main removal mechanisms. As small bubbles rise up, heat transfer and mass transfer occur at the interface and the pressure acting on the bubble also changes. These change the size of bubbles.

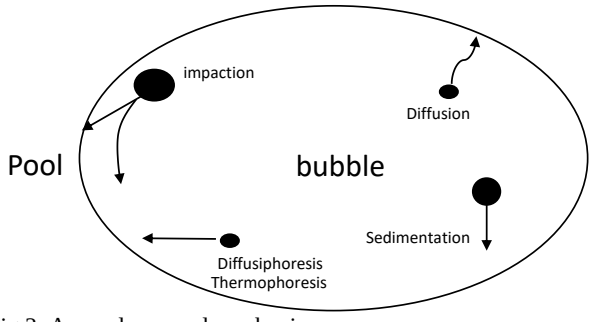

Fig 2. Aerosol removal mechanisms

2.2.1 Bubble formation and velocity

The stable small bubbles are known to have a lognormal size distribution. Although it is realistic to consider all bubbles size with a lognormal distribution, a single diameter was used to represent the swarm region. A diameter of a small bubble was 0.72cm for non-condensable gas injection. When steam is mixed in the bubble, a diameter of the bubbles changes to a formula where the steam fraction is considered [3].

$$d_{bub} = 0.72e^{\left\{2.303\left[-0.2265+(0.0203+0.0313X_{nc})^{\frac{1}{2}}\right]\right\}} \quad (11)$$

For the bubble rise velocity, terminal velocity was used and it has been calculated using Wallis five regime theory [6].

2.2.2 Aerosol removal at bubble rising region

As the broken bubbles rise, aerosols approach to the bubble interface due to Brownian diffusion, inertial impaction, sedimentation, diffusiophoresis, and thermophoresis. Because of this movement, aerosols that existed in the bubble are removed from the pool. The mechanism of removal aerosols can be expressed by following velocity components [2]:

$$U_g = \frac{\rho_p d_p^2 g Cn}{18\mu_g} \quad (12)$$

$$U_{imp} = \frac{9}{4}\frac{{U_B}^2 U_g \sin^2\theta}{R_c g} \quad (13)$$

$$U_{Brow} = 1.8\left(\frac{D_p U_B}{R_c^3}\right)^{0.5}\frac{V}{A_d} \quad (14)$$

$$U_{cond} = \frac{X_s}{X_s+\sum_{i\neq s}X_i\left(\frac{M_i}{M_s}\right)^{0.5}}\frac{-dm_S/dt}{m_s}\frac{\mathrm{V}}{A} \quad (15)$$

$$U_{th} = \frac{3\mu_g}{2\rho_g T_B}\frac{k_h(T_B-T_p)Cn}{K_g}\frac{\frac{K_g}{K_p}+\frac{2.48\lambda_g}{r_p}}{\left(1+\frac{3\lambda_g}{r_p}\right)\left\{1+2\left(\frac{K_g}{K_p}+\frac{2.48\lambda_g}{r_p}\right)\right\}} \quad (16)$$

$$Cn = 1 + 2.493\frac{\lambda_g}{d_p} + 0.84\frac{\lambda_g}{d_p}exp(-0.435\frac{d_p}{\lambda_g}) \quad (17)$$

$$D_p = \frac{kT_B Cn}{3\pi\mu_g d_p} \quad (18)$$

Net deposition velocity consists of five particle capture mechanisms used to define decontamination factor [3].

$$U_{net} = U_g + U_{imp} + U_{Brow} + U_{cond} + U_{th} \quad (19)$$

$$DF_{rise} = \exp\left[\frac{1}{V_b}\int_0^{t_b}\int_A U_{net}dAdt\right] \quad (20)$$

2.2.3 Heat and mass transfer of bubbles

Heat transfer due to the temperature difference between the rising bubbles and pool occurs, which changes the temperature of bubbles. The mass transfer also occurs due to condensation of vapor at the bubble interface. For spherical bubbles, following correlations, dependent on the Reynolds number, are proposed [2].

For $Re < 150$:

$$Sh = 2 + 0.6Re^{\frac{1}{2}}Sc^{\frac{1}{3}} \quad (21)$$

$$Nu = 2 + 0.6Re^{\frac{1}{2}}Pr^{\frac{1}{3}} \quad (22)$$

$Re \geq 150$:

$$Sh = 1.1284\sqrt{\frac{U_B d_E}{D_G}} \quad (23)$$

$$Nu = 1.1284\sqrt{\frac{U_B d_E}{\alpha}} \quad (24)$$

In order to calculate the steam condensation rate, flux of water vapor across a phase change interface was used [2].

$$\frac{dm_s}{dt} = -\frac{M_s P_B}{R_G T_B} k_m A \, ln\left(\frac{1-X_{si}}{1-X_s}\right) \quad (25)$$

A condition at the interface around a bubble has been set to be in equilibrium.

$$X_{si} = \frac{P_{sat}(T_P)}{P_B} \quad (26)$$

3. Result and discussion

3.1 Comparison to POSEIDON-II experiments

Calculated results are compared the POSEIDON-II experiments. POSEIDON-II experiment consists of a number of tests which evaluates the dependence of DF on water height, carrier gas steam mass fraction and particle diameter. The test range of experiment is tabulated in Table 1 [7].

Table 1. POSEIDON-II test range

Pool temperature (°C)	63 ~ 91
Pool height (m)	0.3, 1, 2, 4
Inlet gas flow (kg/h)	87 ~ 153
Inlet steam mass fraction	0 ~ 0.75
Gas temperature (°C)	212 ~ 311
Orifice diameter (cm)	2
Composition	Nitrogen, Steam, SnO_2

Following are assumptions used to simulate the experiment.

- SnO_2 density is 6950 kg/m^3.
- The aerodynamic mass median diameter of the inlet aerosol particle is 0.31 μm.
- Inlet aerosol particle size has a lognormal distribution.
- Globule breaks right after the injection because of the high injection flow rate.

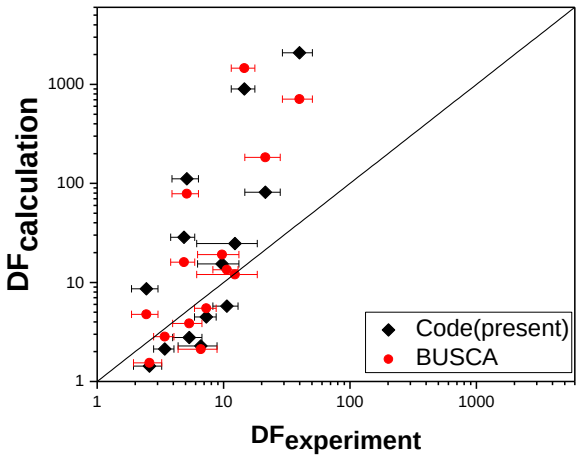

Fig.3 Experimental vs. calculated DF

Figure 3 shows the comparison between the code calculated DF and the experimental DF. In the low DF region, developed code predicts well the experiment. In contrast, in the high DF regions, calculated DFs is much higher than the experimental DFs. Overall, the calculated result a similar trend with the conventional code like BUSCA. The main reason for discrepancies in the BUSCA and the present code may have three reasons. The first reason is due to the bubble. In BUSCA, the diameter of the initial bubble was fixed at 5.6 mm, but the present code uses the correlation according to the steam mole fraction. The second reason is that BUSCA did not consider condensation effect at the injection region, but the present code considers this effect. The third reason is due to aerosol size distribution. There is no information about aerosol size distribution in BUSCA calculation. The size distribution of aerosols is a crucial factor because the diameter of aerosols is very important because it directly affects DF. The deviation at the high DF regions may attribute to the flow regime since such high-velocity condition adopted in the experiment would lead to the Churn-turbulent regime, not a bubbly regime used in the calculation. Therefore, reasonable correlations concerning velocity should be considered to simulate experiments.

4. Conclusion

Pool scrubbing code was developed to calculate aerosol retention in the pool using existing aerosol removal mechanisms. The developed code was compared with the POSEIDON-II experiment. It currently uses terminal velocity correlations and is different from the velocity measured in actual experiments - different flow regime. Further approaches are needed to reflect the real phenomenon.

Notation

Cn	Cunningham slip factor
D_o	injection velocity
D	diffusion coefficient for particle
$D_{cr_{Weber}}$	critical diameter of Weber criterion
$D_{cr_{Levich}}$	critical diameter of Levich criterion
$D_{cr_{Battelle}}$	critical diameter of Battelle
D_G	gas diffusivity
D_g	globule diameter
d_{bub}	bubble diameter
d_p	particle diameter
$DF_{Inj_{imp}}$	DF due to impaction at injection region
$DF_{Inj_{con}}$	DF due to condensation at injection region
$DF_{Inj_{cen}}$	DF due to centrifugal force at injection region
$DF_{Inj_{dif}}$	DF due to diffusion at injection region
$DF_{Inj_{gra}}$	DF due to gravitation at injection region
f	friction factor

k	Boltzmann's constant
K_g	bubble gas thermal conductivity
k_h	heat transfer coefficient
k_m	mass transfer coefficient
K_p	thermal conductivity of the particle
l	characteristic length
Nu	Nusselt number
Pr	Prandtl number
R_c	radius of curvature
Re	Reynolds number
R_G	gas constant
r_p	particle radius
Sc	Schmidt number
Sh	Sherwood number
T_B	bubble temperature
t_b	bubble rise time
t_f	globule filling time
T_p	pool temperature
t_{stop}	stopping time
U_o	injection velocity
U_B	bubble velocity
U_c	centrifugal capture velocity
U_g	gravitational velocity
$V_{Globule}$	globule volume
X_o	mole fraction of non-condensable in the gas after it attains thermal and vapor equilibrium
X_i	mole fraction of non-condensable in inlet gas
X_{nc}	mole fraction of non-condensable gas
X_s	steam mole fraction
α	thermal diffusivity
σ	bubble surface tension
μ_g	gas viscosity
λ_g	mean free path of gas molecules
ρ_g	gas density
ρ_l	pool liquid density
ρ_p	particle density

REFERENCES

[1] 원자력 안전위원회, 사고관리 범위 및 사고 관리능력 평가의 세부기준에 관한 규정안, 2016.
[2] Ramsdale, BUSCA-JUN91 Reference Manual, PSI, 1995.
[3] P. C. Owczarski and K. W. Burk, SPARC-90: a Code for Calculating Fission Product Capture in Suppression Pools, NUREG/CR-5765, 1991.
[4] L.E. Herranz et al., Review and assessment of pool scrubbing models, CIEMAT, 1994
[5] M.Calvoet al., Bubble break-up model, European Communities, 1969.
[6] Graham B. Wallis, One-dimensional Two-phase Flow, McGraw-Hill, 1969
[7] A. Dehbi, D. Suckow, S. Guentay, Aerosol retention in low-subcooling pools under realistic accident conditions, Nuclear Engineering and Design, 2000.
[8] I. Kaneko, M. Fukasawa et al., Experimental study on aerosol removal effect by pool scrubbing, 22nd DOE/NRC nuclear air cleaning and treatment conference, 1992.